



Impact of chamber wall loss of gaseous organic compounds on SOA formation

Y. S. La et al.

This discussion paper is/has been under review for the journal Atmospheric Chemistry and Physics (ACP). Please refer to the corresponding final paper in ACP if available.

Impact of chamber wall loss of gaseous organic compounds on secondary organic aerosol formation: explicit modeling of SOA formation from alkane and alkene oxidation

Y. S. La¹, M. Camredon¹, P. J. Ziemann², R. Valorso¹, A. Matsunaga³,
V. Lannuque¹, J. Lee-Taylor⁴, A. Hodzic⁴, S. Madronich⁴, and B. Aumont¹

¹LISA, UMR CNRS 7583, Université Paris Est Créteil et Université Paris Diderot, 94010 Créteil CEDEX, France

²Department of Chemistry and Biochemistry and Cooperative Institute for Research in Environmental Sciences (CIRES), University of Colorado, Boulder, Colorado, USA

³Air Pollution Research Center, University of California, Riverside, California, USA

⁴National Center for Atmospheric Research, Boulder, Colorado, USA

Title Page

Abstract

Introduction

Conclusions

References

Tables

Figures



Back

Close

Full Screen / Esc

Printer-friendly Version

Interactive Discussion



Received: 28 July 2015 – Accepted: 7 August 2015 – Published: 3 September 2015

Correspondence to: B. Aumont (bernard.aumont@lisa.u-pec.fr)

Published by Copernicus Publications on behalf of the European Geosciences Union.

ACPD

15, 23893–23930, 2015

Impact of chamber wall loss of gaseous organic compounds on SOA formation

Y. S. La et al.

Title Page

Abstract

Introduction

Conclusions

References

Tables

Figures



Back

Close

Full Screen / Esc

Printer-friendly Version

Interactive Discussion



Abstract

Recent studies have shown that low volatility gas-phase species can be lost onto the smog chamber wall surfaces. Although this loss of organic vapors to walls could be substantial during experiments, its effect on secondary organic aerosol (SOA) formation has not been well characterized and quantified yet. Here the potential impact of chamber walls on the loss of gaseous organic species and SOA formation has been explored using the Generator for Explicit Chemistry and Kinetics of the Organics in the Atmosphere (GECKO-A) modeling tool which explicitly represents SOA formation and gas/wall partitioning. The model was compared with 41 smog chamber experiments of SOA formation under OH oxidation of alkane and alkene series (linear, cyclic and C₁₂-branched alkanes and terminal, internal and 2-methyl alkenes with 7 to 17 carbon atoms) under high NO_x conditions. Simulated trends match observed trends within and between homologous series. The loss of organic vapors to the chamber walls is found to affect SOA yields as well as the composition of the gas and the particle phases. Simulated distributions of the species in various phases suggest that nitrates, hydroxynitrates and carbonylestere could substantially be lost onto walls. The extent of this process depends on the rate of gas/wall mass transfer, the vapor pressure of the species and the duration of the experiments. This work suggests that SOA yields inferred from chamber experiments could be underestimated up to 0.35 yield unit due to the loss of organic vapors to chamber walls.

1 Introduction

Secondary organic aerosols (SOA) represent a major fraction of the fine particulate matter mass (e.g. Jimenez et al., 2009), thus contributing to the physicochemical properties of aerosols and to their impact on human health, climate and visibility. SOA are produced by condensation of low volatile organic species formed during gaseous oxidation of emitted volatile and intermediate volatility organic compounds (VOC and IVOC)

Impact of chamber wall loss of gaseous organic compounds on SOA formation

Y. S. La et al.

Title Page

Abstract

Introduction

Conclusions

References

Tables

Figures



Back

Close

Full Screen / Esc

Printer-friendly Version

Interactive Discussion



phase are represented by a first order rate constant (called k_{gw} and k_{wg} respectively hereafter, see Fig. 1) and (ii) the gas/wall partitioning equilibrium follows the Raoult's law, walls being treated as a phase into which the organic compounds can partition. The rate constants are thus linked according to the following equation:

$$\frac{k_{gw}}{k_{wg}} = \frac{RT}{P^{\text{vap}}} \times \left(\frac{C_w}{M_w \gamma_w} \right) \quad (1)$$

where R is the ideal gas constant, T is the temperature and P^{vap} is the vapor pressure of the species. C_w and M_w are an equivalent organic aerosol mass concentration and an equivalent organic aerosol mean molar weight associated with the Teflon film, and γ_w is the activity coefficient of the species in the Teflon film. Values for $C_w/(M_w \gamma_w)$ are empirically derived from chamber observations and Matsunaga and Ziemann (2010) reported values of 9, 20, 50 and 120 $\mu\text{mole m}^{-3}$ for n -alkanes, 1-alkenes, 2-alcohols and 2-ketones respectively.

This wall loss is in competition with gas/particle partitioning (see Fig. 1) and the distribution of organic compounds between the gas phase, the particle phase and the walls depends also on the characteristic times associated with the gas/particle mass transfer. Assuming the sorption of gaseous organic species to the particle to be limited by gas phase diffusion, the first order loss rate of gaseous organic species to the particle, k_{gp} , can be expressed as:

$$k_{gp} = 4\pi D_g r_p C_p \quad (2)$$

where D_g is the species gas phase diffusivity, r_p the particle radius and C_p the number of particles per unit volume of air (e.g. Seinfeld and Pandis, 2006). At thermodynamic equilibrium, the gas-particle partitioning is expected to follow the Raoult's law (e.g. Pankow, 1994). The rate constants are thus linked according to the following equation:

$$\frac{k_{gp}}{k_{pg}} = \frac{RT}{P^{\text{vap}}} \times \frac{C_{\text{aer}}}{M_{\text{aer}} \gamma_{\text{aer}}} \quad (3)$$

Impact of chamber wall loss of gaseous organic compounds on SOA formation

Y. S. La et al.

Title Page

Abstract

Introduction

Conclusions

References

Tables

Figures

◀

▶

◀

▶

Back

Close

Full Screen / Esc

Printer-friendly Version

Interactive Discussion



Impact of chamber wall loss of gaseous organic compounds on SOA formation

Y. S. La et al.

Title Page

Abstract

Introduction

Conclusions

References

Tables

Figures

◀

▶

◀

▶

Back

Close

Full Screen / Esc

Printer-friendly Version

Interactive Discussion



under 10^{-7} atm. For high volatility species, equilibrium is achieved on a short time scale (below 6 min): the gas/particle/wall partitioning is under a thermodynamic control. By contrast, for low volatility species, the distributions change with time and the gas/particle/wall partitioning is under kinetic control. Wall loss is thus expected to significantly impact SOA measurements, being in competition with the gas/particle partitioning of SVOC and acting as a sink for gaseous intermediates that ultimately produce SOA contributors after additional oxidation steps.

The objectives of this study are (i) to quantify the potential impact of chamber walls on the loss of gaseous organics and therefore SOA formation, (ii) to explore the structure of organic species mainly impacted by this loss and (iii) to assess our current understanding of SOA formation from various structures of VOC and IVOC. The methodology used here consists of simulating a selected set of experiments using an explicit description of SOA formation (i.e. gaseous oxidation and gas/particle partitioning). The Generator for Explicit Chemistry and Kinetics of the Organics in the Atmosphere (GECKO-A) (e.g. Aumont et al., 2005; Camredon et al., 2007; Valorso et al., 2011) has been used to generate the explicit gaseous chemical schemes and the properties required to describe the gas/particle partitioning (i.e. the saturation vapor pressure of all species). Alkanes and alkenes are an important class of compounds to study fundamental chemical reactions involved in atmospheric oxidation and the effects of molecular structure on the formation of low volatility compounds which could form SOA. The set of smog chamber experiments performed in the Ziemann lab at the UC-Riverside Air Pollution Research Center (APRC) has been selected as it includes a large set of alkane and alkene structures (of varying carbon chain length and including cyclic, linear and branched species) (e.g. Lim and Ziemann, 2009a, b; Matsunaga et al., 2009). Furthermore, the Matsunaga et al. parameterizations of gaseous organic species wall loss have been fitted for this specific chamber (e.g. Matsunaga and Ziemann, 2010). Experimental conditions are described in Sect. 2. Section 3 is devoted to describing the modeling tool and setup. In Sect. 4, the results of the comparison between the measured

and simulated SOA yields are presented and the GECKO-A chemical mechanisms are used to identify SOA products likely affected the by gas/wall partitioning process.

2 Experimental conditions

The experimental dataset includes linear, branched and cyclic alkanes, linear and 2-methyl 1-alkenes and internal alkenes with a number of carbon atoms ranging from 7 to 17. All the experiments were performed in the UC-Riverside APRC chamber under high NO_x conditions (5–10 ppm), dry conditions ($\text{RH} < 1\%$) and at ambient temperature. The CH_3ONO photolysis was used to produce OH radicals. Organic seeds were introduced to enhance gas-to-particle partitioning. Experiments were typically carried out with 1 ppm of hydrocarbon (0.5 ppm for precursors with 17 carbon atoms), 5 or 10 ppm each of CH_3ONO and NO and 200–400 $\mu\text{g m}^{-3}$ of DOS (dioctylsebacate) as organic seeds. The precursors and initial seeds were introduced into the chamber and let in the dark to achieve gas/wall partitioning equilibrium. The oxidation starts when the black light lamps are turned on to initiate the CH_3ONO photolysis. A detailed description of these experiments can be found in Lim and Ziemann (2009b), Matsunaga (2009) and Matsunaga et al. (2009). Initial conditions of the experiments are summarized in Table 1.

3 Model description and simulation setup

3.1 Gaseous and condensed phase chemical schemes

An explicit description of long chain hydrocarbon oxidation processes up to the final production of CO_2 involves millions of reactions (e.g. Aumont et al., 2005). Such explicit chemical schemes are too large to be written manually. The GECKO-A computer program has been developed to overcome this difficulty. This tool is used here to generate explicit chemical schemes for the long chain hydrocarbons.

23900

ACPD

15, 23893–23930, 2015

Impact of chamber wall loss of gaseous organic compounds on SOA formation

Y. S. La et al.

Title Page

Abstract

Introduction

Conclusions

References

Tables

Figures

◀

▶

◀

▶

Back

Close

Full Screen / Esc

Printer-friendly Version

Interactive Discussion



sion of their gaseous chemistry in the chemical schemes is thus not needed. Gaseous reactions were not considered in the chemical schemes for species having a vapor pressure lower than 10^{-13} atm, being negligible in the gaseous phase under these experimental conditions (C_{aer} varying between 100 and $6000 \mu\text{g m}^{-3}$). Gas/particle and gas/wall mass transfers were considered for stable (i.e. non radical) species only. Figure 4 shows the number of stable and total organic species in these reduced chemical schemes as a function of the number of carbon atoms in the parent compound for the studied precursor's families.

3.4 Simulation setup

The explicit chemical schemes generated by GECKO-A were implemented in a box model. Time integration of chemical schemes and mass transfers is solved using the two-step solver (Verwer et al., 1994, 1996). Photolysis frequencies for inorganic and organic species for a black light spectrum were calculated using cross section and quantum yields described in Aumont et al. (2005). The photolysis of methyl nitrite was calculated using a quantum yield equal to 0.33 (Heicklen, 1988) and the absorption cross section measured by Taylor et al. (1986). All the photolysis frequencies were scaled based on the measured J_{NO_2} . Simulations were initialized with the measured concentrations listed in Table 1. Similar to the experimental conditions, a 60 min period in the dark is first simulated to enforce gas/wall equilibrium for the parent hydrocarbon before starting the oxidation.

Simulated temporal evolutions of the decays of *n*-alkane in the gas phase are represented in Fig. 5 with and without considering gas/wall partitioning. Linear alkanes having more than 13 carbon atoms show a drop in the gaseous concentration early in the simulation mainly due to the chamber wall partitioning. As expected, this drop increases with the chain length due to the decrease of vapor pressure. Similar trends are observed for the other series of precursors. These behaviors indicate that a significant fraction of the initial hydrocarbon load can be removed into the wall for IVOC precursors. Besides it is noteworthy that for these species the gas/wall partitioning equilibrium

Impact of chamber wall loss of gaseous organic compounds on SOA formation

Y. S. La et al.

Title Page

Abstract

Introduction

Conclusions

References

Tables

Figures



Back

Close

Full Screen / Esc

Printer-friendly Version

Interactive Discussion



is achieved within a few minutes, a timescale short enough to not observe that process during most of chamber experiments.

The concentration of the parent hydrocarbon was measured at the end of each experiment and the mass of reacted hydrocarbon ΔHC (defined as the difference between the initial and final gas phase concentrations) was used to assess the simulation setup. Figure 6 shows the comparison between the measured and simulated ΔHC mass. The values are displayed by chemical family and as a function of carbon chain length or number of methyl groups on the carbon backbone. Within each family, the amount of reacted compound typically grows with the size of the carbon skeleton. This behavior is consistent with the corresponding increase of the hydrocarbon +OH rate constant with the size of the carbon skeleton (e.g. Kwok and Atkinson, 1995). For the whole set of simulations, ΔHC are well reproduced by the model. Hence, the simulation setups are considered suitable to represent experimental conditions.

4 Results and discussions

4.1 Comparison between measured and simulated SOA yields

SOA yield is defined as the ratio of SOA mass produced to the mass of reacted hydrocarbon (ΔHC). A comparison of the experimental and the simulated final SOA yields is presented in Fig. 7. Results are reported as a function of the number of carbon atoms or branching in the parent hydrocarbon. Experimental data are displayed as given in the experimental papers by Lim and Ziemann (2009b), Matsunaga (2009) and Matsunaga et al. (2009).

Simulations were performed with and without wall loss taken into account for the organic vapors (see Fig. 7). Simulations reported in Fig. 7 were obtained using $C_w/(M_w\gamma_w) = 120 \mu\text{mole m}^{-3}$ for all secondary species and using for τ_{gw} 10, 30 and 60 min. Similar results were obtained for the simulations performed with $C_w/(M_w\gamma_w) = 50 \mu\text{mole m}^{-3}$ (see Fig. S1 in the Supplement). Simulations presented in Fig. 7 were

Impact of chamber wall loss of gaseous organic compounds on SOA formation

Y. S. La et al.

Title Page

Abstract

Introduction

Conclusions

References

Tables

Figures



Back

Close

Full Screen / Esc

Printer-friendly Version

Interactive Discussion



Impact of chamber wall loss of gaseous organic compounds on SOA formation

Y. S. La et al.

Title Page

Abstract

Introduction

Conclusions

References

Tables

Figures

◀

▶

◀

▶

Back

Close

Full Screen / Esc

Printer-friendly Version

Interactive Discussion



carried out using the SAR developed by Atkinson (2007) to describe the alkoxy chemistry (hereafter denoted ATK simulations). A set of simulations was also performed using the Vereecken and Peeters SARs for the estimation of the alkoxy decomposition rates (2009) and the alkoxy isomerization rates (2010) (hereafter denoted VER simulations). Figure S2 in the Supplement shows the comparison of the results obtained with ATK and VER, which is discussed below.

For the alkane series, the experimental trends are well captured by the model. In particular, both the simulated and observed SOA yields (i) increase with the carbon number of the precursor, (ii) are higher for a cyclic compared to a linear structure and (iii) decrease with the number of methyl groups on the carbon skeleton. This behavior is mostly driven by the fate of alkoxy radicals. While decomposition (i.e. C-C bond breaking) pathways of linear alkoxy radicals lead to molecules with smaller carbon backbone (see Fig. 9), the decomposition of cyclic alkoxy radicals preserves the size of the carbon backbone. Similarly, decomposition is enhanced for branched alkoxy radicals (e.g. Lim and Ziemann et al., 2009a). This effect is well represented in the simulations, as discussed in Aumont et al. (2013). Figure 7 shows that the SOA yields simulated without wall loss taken into account are systematically overestimated. A better agreement is obtained when the partitioning of organic species to the wall is considered in the model. Decreasing characteristic time of the gas to wall mass transfer decreases the simulated SOA yields (see Fig. 7). Best agreement is obtained for the lower value of τ_{gw} (10 min) with reductions ranging from 0.05 to 0.35 yield units. Note that a change in gas/wall equilibrium value does not affect these results (see Fig. S1). Besides, using the lower value of $C_{\text{w}}/(M_{\text{w}}\gamma_{\text{w}})$ ($50 \mu\text{mole m}^{-3}$) increases SOA yield by less than 15% (see Fig. S1). As discussed above, for a simulation lasting 1 h, the gas/particle partitioning outweighs the gas/wall partitioning for low volatility species, leading to a rather low sensitivity of the wall properties. Partitioning is therefore rather under the kinetic control than thermodynamic control.

The experimental trends are also well captured by the model for the alkene series. Simulations and experimental observations show that SOA yields (i) increase with the

Impact of chamber wall loss of gaseous organic compounds on SOA formation

Y. S. La et al.

Title Page

Abstract

Introduction

Conclusions

References

Tables

Figures



Back

Close

Full Screen / Esc

Printer-friendly Version

Interactive Discussion



the oxidation of terminal, internal and 2-methyl alkenes. The VER configuration leads to a larger fraction of decomposition than the ATK configuration, which is consistent with a lower simulated SOA yields for the VER configuration compared to the ATK one. Table 2 also reports experimentally derived branching ratios from measurements of the oxidation products (Matsunaga et al., 2009; Aschmann et al., 2010; Ziemann, 2011). These experimental results suggest that the isomerization routes are underestimated in both the ATK and VER configurations for OH + alkene systems.

4.2 Gas/wall partitioning impacts on SOA composition

Simulations performed with the GECKO-A mechanisms were used to examine which species are prone to partition with the chamber walls. Figure 8 presents the distribution of the top fifteen species in the gas, particles and wall (i.e. Teflon) phases for various experiments. Simulated results are reported at the end of the experiments in mass concentrations (in $\mu\text{g m}^{-3}$ of air or equivalent for the Teflon phase) for both cases: without (left panel) and with partitioning to the wall using $\tau_{\text{gw}} = 10$ min and $C_{\text{w}}/(M_{\text{w}}\gamma_{\text{w}}) = 120 \mu\text{mole m}^{-3}$ (right panel). Results in Fig. 8 are reported for *n*-octane (C_8), *n*-dodecane (C_{12}) and *n*-hexadecane (C_{16}) to examine the effects of chain length on mass distribution.

In Fig. 8, species are categorized based on organic moieties (isomers having identical functional groups are lumped together), and whether the species are produced by functionalization (with number of generation) or by decomposition routes. The letter code given in Fig. 9 for each category denotes the functional groups on the carbon backbones (N = nitrate, O = alcohol, K = ketone, D = aldehyde, E = ether, P = peroxyacetyl nitrate, S = ester U = carbon double bond) or characteristics of the carbon backbone (T = cyclic structure, C = saturated aliphatic hydrocarbon – here the parent compound). A generic chemical mechanism leading to this set of species is presented in Fig. 9, with the codes corresponding to the various chemical structures.

chemical reactions are involved in the oxidation of long chain alkanes, leading to the same families of species but with decreasing volatility when the size of the carbon skeleton increases. The vapor pressures of the major chemical families simulated during the alkane experiments are given as a function of the number of carbon atom (n_C) in the backbone in Fig. 10. The shaded grey area corresponds to the volatility domain where significant partitioning to the walls is expected after 1 h (i.e. 10^{-8} – 10^{-5} atm, see introduction).

The location of a given family in this volatility/ n_C framework largely explains the wall effect highlighted in Fig. 8. For example for the alkyl nitrate family (N), a first generation product, (i) C_8 species appear to be too volatile to partition to the condensed particle phase (those are located on the right side of the grey area), (ii) C_{12} species are volatile enough to partition to the wall but not enough to substantially partition to the particles (even if no wall is considered) and (iii) C_{16} species are mostly found in the condensed phase but the volatility is not low enough to prevent a substantial partitioning to the wall (those are still on the volatility domain where the walls substantially impact the species distributions). The mass reductions due to gas/wall partitioning for C_8 , C_{12} and C_{16} alkyl nitrates are respectively -2 , -40 and -7% in the gas phase and -63 and -26% in the particle phase for C_{12} and C_{16} species, respectively. Compared to the nitrate family, the volatility of the hydroxynitrates (NO), also first generation products, is shifted toward lower volatility (typically by a factor of 30). For that NO family, C_8 species partition to the walls to more than 50 % (but not into the particles) affecting gas composition while C_{16} species are almost exclusively found in the particle phase, owing to their low volatility and the resulting kinetic control of the partitioning (see introduction). For C_{12} hydroxynitrates, 50 % of the mass is lost into the walls modifying both gas and particle concentrations. The behavior of the first generation of cyclic hemiacetals (TOE) is similar to the nitrate family but most second generation species behave rather like the hydroxynitrate family, e.g. the dinitrates (NN) or the DHF oxidation products (TNOE, DS). The deposition of vapor to the walls during the experiments therefore splits a spe-

Impact of chamber wall loss of gaseous organic compounds on SOA formation

Y. S. La et al.

Title Page

Abstract

Introduction

Conclusions

References

Tables

Figures

◀

▶

◀

▶

Back

Close

Full Screen / Esc

Printer-friendly Version

Interactive Discussion



Impact of chamber wall loss of gaseous organic compounds on SOA formation

Y. S. La et al.

Title Page

Abstract

Introduction

Conclusions

References

Tables

Figures



Back

Close

Full Screen / Esc

Printer-friendly Version

Interactive Discussion



hemicetals and dihydrofurans coming from the fast cyclization of 1,4-hydroxycarbonyls in the particle. Second generation species are also found to be substantial contributors to SOA. These species are produced from OH oxidation and lead to additional functional groups (mostly nitrate, alcohol or carbonyl) on the carbon backbone. The presence of acid carboxylic esters (AS) and cyclic dinitrate ethers (TNNE) among the major simulated products suggests that DHF oxidation by O₃ and NO₃ can compete with OH oxidation during these experiments. Simulated distributions of the species in the various phases suggest that substantial amounts of nitrates, hydroxynitrates and carbonylestes could be lost onto the walls.

For the alkene series, the simulated SOA yields exhibit a strong dependence on the structure activity relationship used to estimate the fate of the alkoxy radicals. The gas/wall partitioning process cannot fully explain the discrepancies between the model and the observations. Some chemical pathways are clearly missing in the GECKO-A mechanism, e.g. dimers formation and/or heterogeneous oxidation in the particle phase. Thus, further investigations of SOA composition are required.

This work suggests that SOA yields inferred from chamber experiments could be substantially underestimated due to the loss of organic vapors to the wall of the chamber. This process also likely alters the inferred SOA composition. The gas/wall partitioning of organic compounds needs to be routinely characterized for smog chamber data and derived SOA yields. These characterizations appear to be a critical issue to support the development of SOA parameterizations for air quality and climate models based on experimental observations in atmospheric chambers.

The Supplement related to this article is available online at doi:10.5194/acpd-15-23893-2015-supplement.

Acknowledgements. This research work has been supported by the French National Research Agency (ANR) within the ONCEM (ANR-12-BS06-0017) and MAGNIFY (ANR-14-CE01-0010) projects and the French National institute for Geophysical Research (CNRS-INSU) within the LEFE-CHAT program through the Dodec-AOS project.

PJZ acknowledges support from the National Science Foundation (NSF) under grants AGS-1219508 and AGS-1420007.

References

Aschmann, S. M., Tuazon, E. C., Arey, J., and Atkinson, R.: Products and mechanisms of the gas-phase reactions of OH radicals with 1-octene and 7-tetradecene in the presence of NO, *Environ. Sci. Technol.*, 44, 3825–3831, doi:10.1021/es100550n, 2010.

Aschmann, S. M., Arey, J., and Atkinson, R.: Kinetics and products of the reaction of OH radicals with 3-methoxy-3-methyl-1-butanol., *Environ. Sci. Technol.*, 45, 6896–6901, doi:10.1021/es201475g, 2011.

Atkinson, R.: Rate constants for the atmospheric reactions of alkoxy radicals: an updated estimation method, *Atmos. Environ.*, 41, 8468–8485, doi:10.1016/j.atmosenv.2007.07.002, 2007.

Atkinson, R. and Arey, J.: Atmospheric degradation of volatile organic compounds, *Chem. Rev.*, 103, 4605–4638, doi:10.1021/cr0206420, 2003.

Atkinson, R., Arey, J., and Aschmann, S. M.: Atmospheric chemistry of alkanes: review and recent developments, *Atmos. Environ.*, 42, 5859–5871, doi:10.1016/j.atmosenv.2007.08.040, 2008.

Aumont, B., Szopa, S., and Madronich, S.: Modelling the evolution of organic carbon during its gas-phase tropospheric oxidation: development of an explicit model based on a self generating approach, *Atmos. Chem. Phys.*, 5, 2497–2517, doi:10.5194/acp-5-2497-2005, 2005.

Aumont, B., Valorso, R., Mouchel-Vallon, C., Camredon, M., Lee-Taylor, J., and Madronich, S.: Modeling SOA formation from the oxidation of intermediate volatility *n*-alkanes, *Atmos. Chem. Phys.*, 12, 7577–7589, doi:10.5194/acp-12-7577-2012, 2012.

Aumont, B., Camredon, M., Mouchel-Vallon, C., La, S., Ouzebidour, F., Valorso, R., Lee-Taylor, J., and Madronich, S.: Modeling the influence of alkane molecular structure on sec-

Impact of chamber wall loss of gaseous organic compounds on SOA formation

Y. S. La et al.

Title Page

Abstract

Introduction

Conclusions

References

Tables

Figures

◀

▶

◀

▶

Back

Close

Full Screen / Esc

Printer-friendly Version

Interactive Discussion



Impact of chamber wall loss of gaseous organic compounds on SOA formation

Y. S. La et al.

Title Page

Abstract

Introduction

Conclusions

References

Tables

Figures



Back

Close

Full Screen / Esc

Printer-friendly Version

Interactive Discussion

Jimenez, J. L., Canagaratna, M. R., Donahue, N. M., Prevot, A. S., Zhang, Q., Kroll, J. H., De Carlo, P. F., Allan, J. D., Coe, H., Ng, N. L., Aiken, A. C., Docherty, K. S., Ulbrich, I. M., Grieshop, A. P., Robinson, A. L., Duplissy, J., Smith, J. D., Wilson, K. R., Lanz, V. A., Hueglin, C., Sun, Y. L., Tian, J., Laaksonen, A., Raatikainen, T., Rautiainen, J., Vaattovaara, P., Ehn, M., Kulmala, M., Tomlinson, J. M., Collins, D. R., Cubison, M. J., Dunlea, E. J., Huffman, J. A., Onasch, T. B., Alfarra, M. R., Williams, P. I., Bower, K., Kondo, Y., Schneider, J., Drewnick, F., Borrmann, S., Weimer, S., Demerjian, K., Salcedo, D., Cottrell, L., Griffin, R., Takami, A., Miyoshi, T., Hatakeyama, S., Shimono, A., Sun, J. Y., Zhang, Y. M., Dzepina, K., Kimmel, J. R., Sueper, D., Jayne, J. T., Herndon, S. C., Trimborn, A. M., Williams, L. R., Wood, E. C., Middlebrook, A. M., Kolb, C. E., Baltensperger, U., and Worsnop, D. R.: Evolution of organic aerosols in the atmosphere, *Science*, 326, 1525–1529, doi:10.1126/science.1180353, 2009.

Kjaergaard, H. G., Knap, H. C., Ørnsø, K. B., Jørgensen, S., Crounse, J. D., Paulot, F., and Wennberg, P. O.: Atmospheric fate of methacrolein. 2. Formation of lactone and implications for organic aerosol production, *J. Phys. Chem. A*, 116, 5763–5768, doi:10.1021/jp210853h, 2012.

Kokkola, H., Yli-Pirilä, P., Vestnerinen, M., Korhonen, H., Keskinen, H., Romakkaniemi, S., Hao, L., Kortelainen, A., Joutsensaari, J., Worsnop, D. R., Virtanen, A., and Lehtinen, K. E. J.: The role of low volatile organics on secondary organic aerosol formation, *Atmos. Chem. Phys.*, 14, 1689–1700, doi:10.5194/acp-14-1689-2014, 2014.

Kroll, J. H. and Seinfeld, J. H.: Chemistry of secondary organic aerosol: formation and evolution of low-volatility organics in the atmosphere, *Atmos. Environ.*, 42, 3593–3624, doi:10.1016/j.atmosenv.2008.01.003, 2008.

Kwok, E. S. C. and Atkinson, R.: Estimation of hydroxyl radical reaction rate constants for gas-phase organic compounds using a structure–reactivity relationship: an update, *Atmos. Environ.*, 29, 1685–1695, doi:10.1016/1352-2310(95)00069-B, 1995.

Lee-Taylor, J., Hodzic, A., Madronich, S., Aumont, B., Camredon, M., and Valorso, R.: Multiday production of condensing organic aerosol mass in urban and forest outflow, *Atmos. Chem. Phys.*, 15, 595–615, doi:10.5194/acp-15-595-2015, 2015.

Lim, Y. B. and Ziemann, P. J.: Products and mechanism of secondary organic aerosol formation from reactions of *n*-alkanes with OH radicals in the presence of NO_x, *Environ. Sci. Technol.*, 39, 9229–9236, doi:10.1021/es051447g, 2005.

Impact of chamber wall loss of gaseous organic compounds on SOA formation

Y. S. La et al.

Title Page

Abstract

Introduction

Conclusions

References

Tables

Figures



Back

Close

Full Screen / Esc

Printer-friendly Version

Interactive Discussion

- Lim, Y. B. and Ziemann, P. J.: Chemistry of secondary organic aerosol formation from OH radical-initiated reactions of linear, branched, and cyclic alkanes in the presence of NO_x , *Aerosol Sci. Tech.*, 43, 604–619, doi:10.1080/02786820902802567, 2009a.
- Lim, Y. B. and Ziemann, P. J.: Effects of molecular structure on aerosol yields from OH radical-initiated reactions of linear, branched, and cyclic alkanes in the presence of NO_x , *Environ. Sci. Technol.*, 43, 2328–2334, doi:10.1021/es803389s, 2009b.
- Lim, Y. B. and Ziemann, P. J.: Kinetics of the heterogeneous conversion of 1,4-hydroxycarbonyls to cyclic hemiacetals and dihydrofurans on organic aerosol particles, *Phys. Chem. Chem. Phys.*, 11, 8029–8039, doi:10.1039/b904333k, 2009c.
- Loza, C. L., Chan, A. W. H., Galloway, M. M., Keutsch, F. N., Flagan, R. C., and Seinfeld, J. H.: Characterization of vapor wall loss in laboratory chambers, *Environ. Sci. Technol.*, 44, 5074–5078, doi:10.1021/es100727v, 2010.
- Martin, P., Tuazon, E. C., Aschmann, S. M., Arey, J., and Atkinson, R.: Formation and atmospheric reactions of 4,5-dihydro-2-methylfuran, *J. Phys. Chem. A*, 106, 11492–11501, doi:10.1021/jp021499h, 2002.
- Matsunaga, A.: Secondary organic aerosol formation from radical-initiated reactions of alkenes: development of mechanisms, PhD thesis, University of California, Riverside, CA, 2009.
- Matsunaga, A. and Ziemann, P. J.: Gas-wall partitioning of organic compounds in a teflon film chamber and potential effects on reaction product and aerosol yield measurements, *Aerosol Sci. Tech.*, 44, 881–892, doi:10.1080/02786826.2010.501044, 2010.
- Matsunaga, A., Docherty, K. S., Lim, Y. B., and Ziemann, P. J.: Composition and yields of secondary organic aerosol formed from OH radical-initiated reactions of linear alkenes in the presence of NO_x : modeling and measurements, *Atmos. Environ.*, 43, 1349–1357, doi:10.1016/j.atmosenv.2008.12.004, 2009.
- McMurry, P. H. and Grosjean, D.: Gas and aerosol wall losses in teflon film smog chambers, *Environ. Sci. Technol.*, 19, 1176–1182, doi:10.1021/es00142a006, 1985.
- Nannoolal, Y., Rarey, J., Ramjugernath, D., and Cordes, W.: Estimation of pure component properties: Part 1. Estimation of the normal boiling point of non-electrolyte organic compounds via group contributions and group interactions, *Fluid Phase Equilibr.*, 226, 45–63, doi:10.1016/j.fluid.2004.09.001, 2004.
- Nannoolal, Y., Rarey, J., and Ramjugernath, D.: Estimation of pure component properties: Part 3. Estimation of the vapor pressure of non-electrolyte organic compounds

Impact of chamber wall loss of gaseous organic compounds on SOA formation

Y. S. La et al.

[Title Page](#)[Abstract](#)[Introduction](#)[Conclusions](#)[References](#)[Tables](#)[Figures](#)[Back](#)[Close](#)[Full Screen / Esc](#)[Printer-friendly Version](#)[Interactive Discussion](#)

via group contribution and group interactions, *Fluid Phase Equilibr.*, 269, 117–133, doi:10.1016/j.fluid.2008.04.020, 2008.

Pankow, J. F.: An absorption model of the gas/aerosol partitioning involved in the formation of secondary organic aerosol, *Atmos. Environ.*, 28, 189–193, doi:10.1016/1352-2310(94)90094-9, 1994.

Pathak, R. K., Stanier, C. O., Donahue, N. M., and Pandis, S. N.: Ozonolysis of α -pinene at atmospherically relevant concentrations: temperature dependence of aerosol mass fractions (yields), *J. Geophys. Res.-Atmos.*, 112, 1–8, doi:10.1029/2006JD007436, 2007.

Presto, A. A. and Donahue, N. M.: Investigation of alpha-pinene + ozone secondary organic aerosol formation at low total aerosol mass, *Environ. Sci. Technol.*, 40, 3536–3543, doi:10.1021/es052203z, 2006.

Santiago, M., Vivanco, M. G., and Stein, A. F.: Evaluation of CMAQ parameterizations for SOA formation from the photooxidation of α -pinene and limonene against smog chamber data, *Atmos. Environ.*, 56, 236–245, doi:10.1016/j.atmosenv.2012.04.011, 2012.

Seinfeld, J. H. and Pandis, S. N.: *Atmospheric Chemistry and Physics: from Air Pollution to Climate Change*, 2nd edn., Wiley, Hoboken, NJ, 2006.

Taylor, W. D., Allston, T. D., Mascato, M. J., Fazekas, G. B., Kozlowski, R., and Takacs, G. A.: Atmospheric photodissociation lifetimes for nitromethane, methyl nitrite and methyl nitrate, *Int. J. Chem. Kinet.*, 12, 231–240, 1980.

Valorso, R., Aumont, B., Camredon, M., Raventos-Duran, T., Mouchel-Vallon, C., Ng, N. L., Seinfeld, J. H., Lee-Taylor, J., and Madronich, S.: Explicit modelling of SOA formation from α -pinene photooxidation: sensitivity to vapour pressure estimation, *Atmos. Chem. Phys.*, 11, 6895–6910, doi:10.5194/acp-11-6895-2011, 2011.

Vereecken, L. and Peeters, J.: Decomposition of substituted alkoxy radicals – Part I: A generalized structure–activity relationship for reaction barrier heights, *Phys. Chem. Chem. Phys.*, 11, 9062–9074, doi:10.1039/b909712k, 2009.

Vereecken, L. and Peeters, J.: A structure–activity relationship for the rate coefficient of H-migration in substituted alkoxy radicals, *Phys. Chem. Chem. Phys.*, 12, 12608–12620, doi:10.1039/c0cp00387e, 2010.

Verwer, J. G. and van Loon, M.: An evaluation of explicit pseudo-steady-state approximation schemes for stiff ODE systems from chemical kinetics, *J. Comput. Phys.*, 113, 347–352, 1994.

Impact of chamber wall loss of gaseous organic compounds on SOA formation

Y. S. La et al.

Title Page

Abstract

Introduction

Conclusions

References

Tables

Figures

◀

▶

◀

▶

Back

Close

Full Screen / Esc

Printer-friendly Version

Interactive Discussion



- Verwer, J. G., Blom, J. G., van Loon, M., and Spee, E. J.: A comparison of stiff ODE solvers for atmospheric chemistry problems, *Atmos. Environ.*, 30, 49–58, doi:10.1016/1352-2310(95)00283-5, 1996.
- 5 Yeh, G. K. and Ziemann, P. J.: Alkyl nitrate formation from the reactions of C_8 – C_{14} *n*-alkanes with OH radicals in the presence of NO_x : measured yields with essential corrections for gas-wall partitioning, *J. Phys. Chem. A*, 118, 8147–57, doi:10.1021/jp500631v, 2014.
- Zhang, X. and Seinfeld, J. H.: A functional group oxidation model (FGOM) for SOA formation and aging, *Atmos. Chem. Phys.*, 13, 5907–5926, doi:10.5194/acp-13-5907-2013, 2013.
- 10 Zhang, X., Schwantes, R. H., Coggon, M. M., Loza, C. L., Schilling, K. A., Flagan, R. C., and Seinfeld, J. H.: Role of ozone in SOA formation from alkane photooxidation, *Atmos. Chem. Phys.*, 14, 1733–1753, doi:10.5194/acp-14-1733-2014, 2014.
- Zhang, X., Schwantes, R. H., McVay, R. C., Lignell, H., Coggon, M. M., Flagan, R. C., and Seinfeld, J. H.: Vapor wall deposition in Teflon chambers, *Atmos. Chem. Phys.*, 15, 4197–4214, doi:10.5194/acp-15-4197-2015, 2015.
- 15 Ziemann, P. J.: Effects of molecular structure on the chemistry of aerosol formation from the OH-radical-initiated oxidation of alkanes and alkenes, *Int. Rev. Phys. Chem.*, 30, 161–195, doi:10.1080/0144235X.2010.550728, 2011.

Impact of chamber wall loss of gaseous organic compounds on SOA formation

Y. S. La et al.

Title Page

Abstract

Introduction

Conclusions

References

Tables

Figures

◀

▶

◀

▶

Back

Close

Full Screen / Esc

Printer-friendly Version

Interactive Discussion



Table 1. Initial and environmental conditions of the experiments.

Exp.	[HC] ₀ (ppm)	[NO] ₀ (ppm)	[CH ₃ ONO] ₀ (ppm)	[DOS seeds] (μg m ⁻³)	<i>J</i> _{NO₂} (min ⁻¹)/ Time exposure (min)
Linear alkanes ^a (C ₇ –C ₁₇)	1 0.5	10	10	90–400	0.38/60
Cyclic alkanes ^a (C ₆ –C ₁₅)	1	10	10	150–300	0.38/60
Branched alkanes ^a (C ₁₂)	1	10	10	100–200	0.38/60
1-Alkenes ^b (C ₈ –C ₁₇)	1 0.5	5	5	200	0.14/6
Internal alkenes ^b (C ₁₄ –C ₁₇)	1 0.3	5	5	200	0.14/6
2-Methyl-1-alkenes ^c (C ₉ –C ₁₅)	1	5	5	200	0.14/6

^a Lim and Ziemann (2009a), ^b Matsunaga et al. (2009) and ^c Matsunaga (2009).

Impact of chamber wall loss of gaseous organic compounds on SOA formation

Y. S. La et al.

Title Page

Abstract

Introduction

Conclusions

References

Tables

Figures

◀

▶

◀

▶

Back

Close

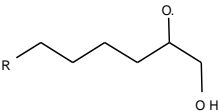
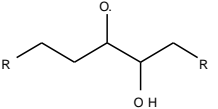
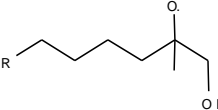
Full Screen / Esc

Printer-friendly Version

Interactive Discussion



Table 2. Decomposition and isomerization branching ratios for selected generic β -hydroxyalkoxy radicals produced from the oxidation of terminal, internal and 2-methyl alkenes as estimated by the ATK and VER configurations of the model and experimentally derived values by Matsunaga et al. (2009), Aschmann et al. (2010), and Ziemann (2011).

	Decomposition/Isomerization branching ratio		
	ATK configuration	VER configuration	Experimental data*
1-alkenes 	0.67/0.33	0.79/0.21	0.45/0.55
Internal alkenes 	1.00/0.00	1.00/0.00	0.67/0.33
2-Methyl-1-alkenes 	0.93/0.07	1.00/0.00	0.59/0.41

* Reported in Ziemann, 2011.

Impact of chamber wall loss of gaseous organic compounds on SOA formation

Y. S. La et al.

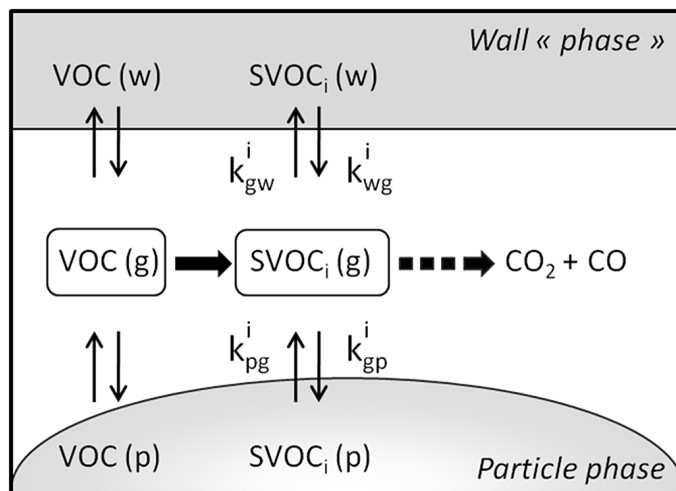


Figure 1. Schematic representation of gas/particle and gas/wall mass transfers of a semi-volatile organic compound (SVOC) produced during gaseous oxidation of VOC.

Title Page

Abstract

Introduction

Conclusions

References

Tables

Figures

◀

▶

◀

▶

Back

Close

Full Screen / Esc

Printer-friendly Version

Interactive Discussion



Impact of chamber wall loss of gaseous organic compounds on SOA formation

Y. S. La et al.

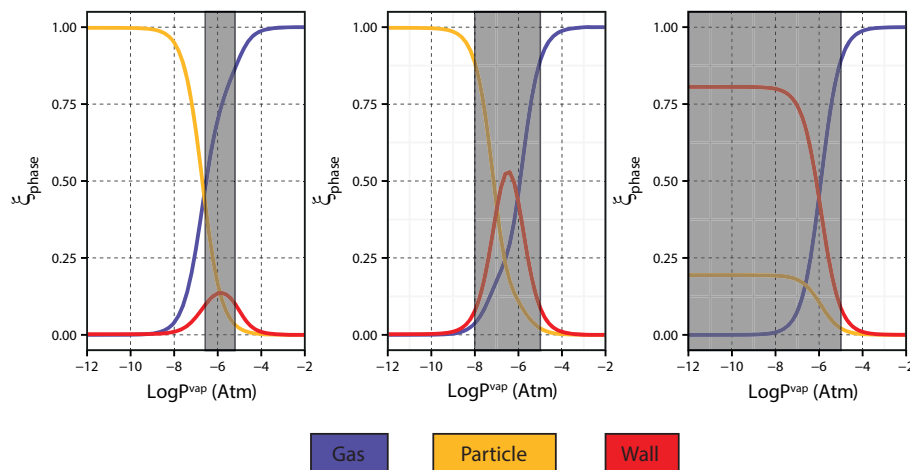


Figure 2. Time evolution of the fraction in the gas, particle and wall phases as a function of the vapor pressure for a continuous distribution of species considered to be initially only in the gas phase. Grey zones represent the volatility range impacted by wall losses at a molar fraction higher than 10%.

Title Page

Abstract

Introduction

Conclusions

References

Tables

Figures

◀

▶

◀

▶

Back

Close

Full Screen / Esc

Printer-friendly Version

Interactive Discussion



Impact of chamber wall loss of gaseous organic compounds on SOA formation

Y. S. La et al.

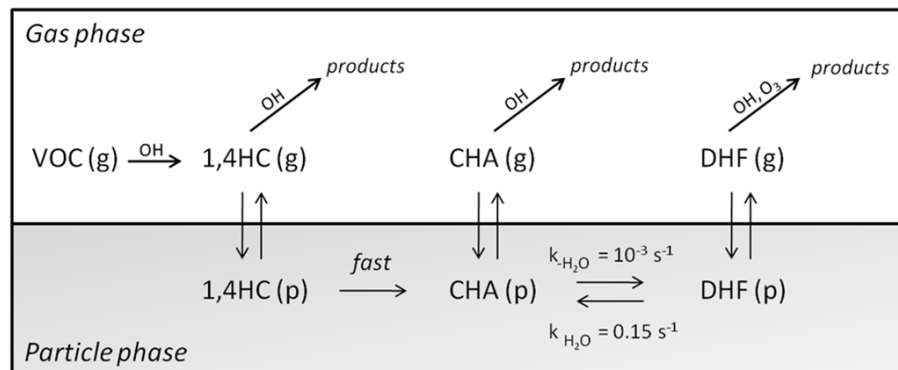


Figure 3. Representation of DHF formation in the GECKO-A protocol.

[Title Page](#)
[Abstract](#)
[Introduction](#)
[Conclusions](#)
[References](#)
[Tables](#)
[Figures](#)
[◀](#)
[▶](#)
[◀](#)
[▶](#)
[Back](#)
[Close](#)
[Full Screen / Esc](#)
[Printer-friendly Version](#)
[Interactive Discussion](#)


Impact of chamber wall loss of gaseous organic compounds on SOA formation

Y. S. La et al.

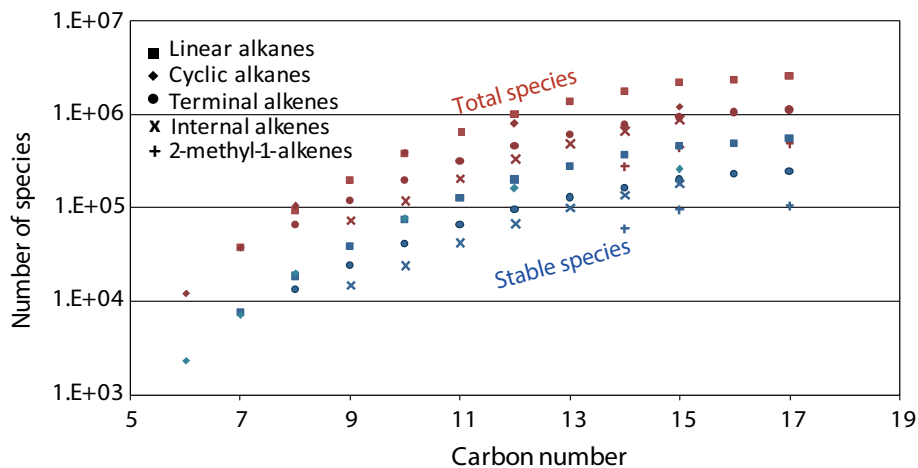


Figure 4. Number of stable (blue) and total organic species (red) in the reduced chemical schemes generated with GECKO-A as a function of the number of carbons in the parent compound for the studied precursor's families.

Impact of chamber wall loss of gaseous organic compounds on SOA formation

Y. S. La et al.

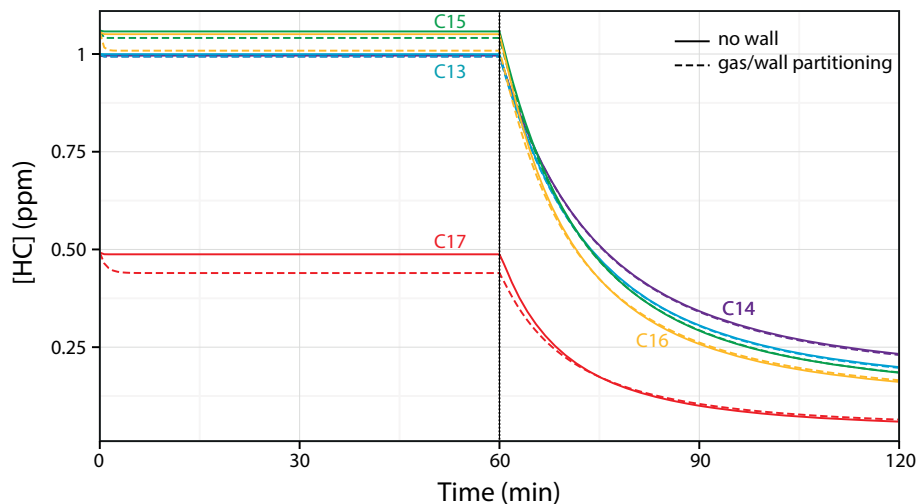


Figure 5. Simulated temporal evolutions of the decays of *n*-alkanes in the gas phase without (solid line) and with (dashed line) gas/wall partitioning. The dotted line at 60 min corresponds to the time at which the lights are turned on.

Impact of chamber wall loss of gaseous organic compounds on SOA formation

Y. S. La et al.

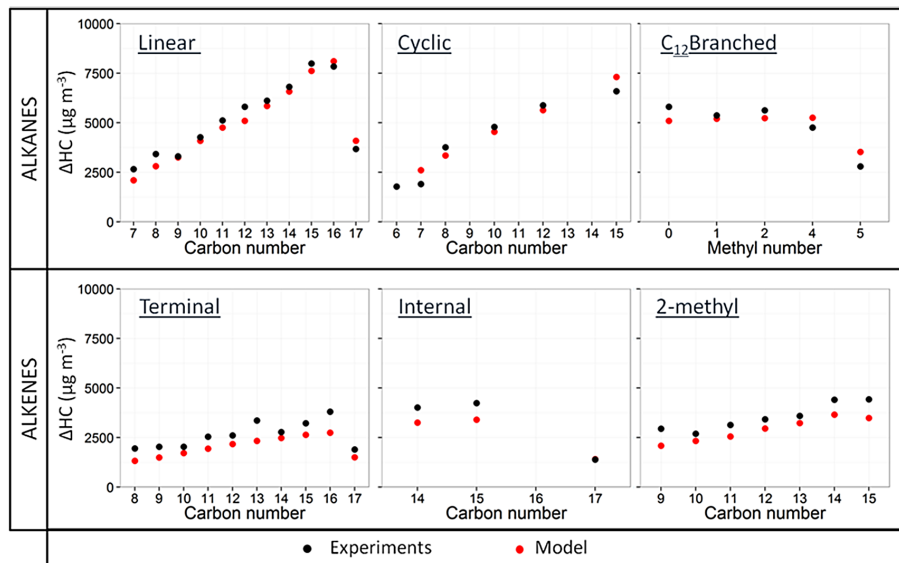


Figure 6. Comparison between the measured (black) and the simulated (red) ΔHC mass for the different chemical families as a function of carbon chain length or number of methyl groups of the carbon backbone.

[Title Page](#)
[Abstract](#)
[Introduction](#)
[Conclusions](#)
[References](#)
[Tables](#)
[Figures](#)
[Back](#)
[Close](#)
[Full Screen / Esc](#)
[Printer-friendly Version](#)
[Interactive Discussion](#)

Impact of chamber wall loss of gaseous organic compounds on SOA formation

Y. S. La et al.

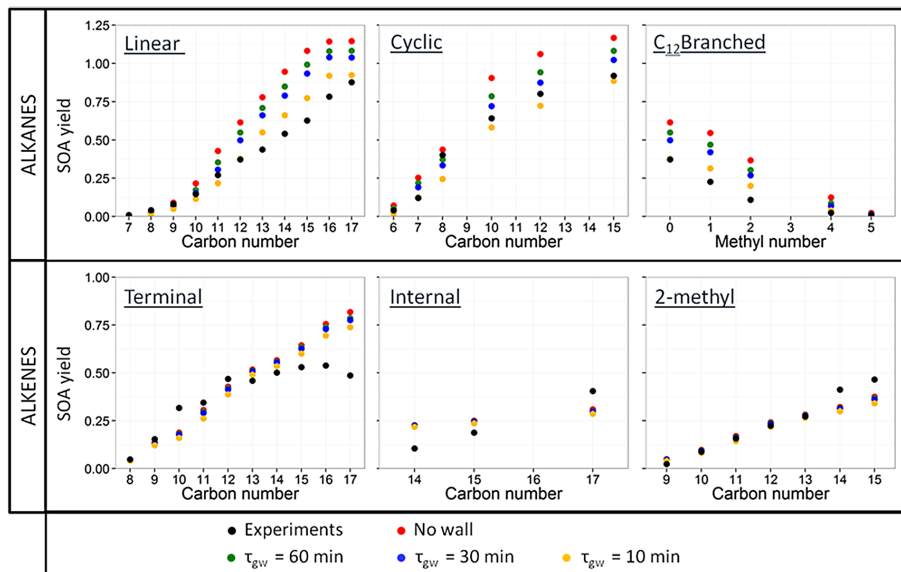


Figure 7. Comparison between measured (black) and simulated SOA yields for the different chemical families as a function of carbon chain length or presence of methyl groups on the carbon backbone. Simulations are shown without wall loss (red) and with wall loss using a value of $C_w/(M_w Y_w) = 120 \mu\text{mole m}^{-3}$ for all secondary species and a τ_{gw} of 10 min (yellow), 30 min (blue) or 60 min (green).

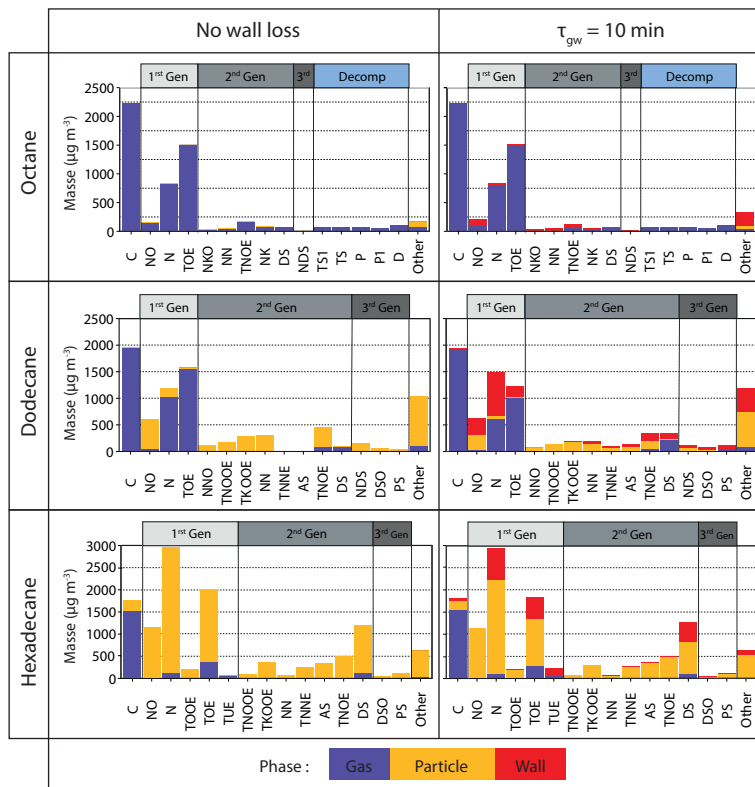


Figure 8. Distribution of the top fifteen species between the gas phase (purple), the particle phase (yellow) and the walls (red) at the end of the simulations for *n*-octane (C_8), *n*-dodecane (C_{12}) and *n*-hexadecane (C_{16}). Simulated results are reported in mass concentrations (in $\mu\text{g m}^{-3}$ of air or equivalent for the Teflon phase) for simulations conducted without wall loss (left panel) and with partitioning to the wall using $\tau_{\text{gw}} = 10$ min and $C_w/(M_w\gamma_w) = 120 \mu\text{mole m}^{-3}$ (right panel).

